

OPTIMAL SPEED AND TORQUE ESTIMATION FOR IMPROVING THE DTC
DYNAMIC PERFORMANCE OF INDUCTION MACHINES

IBRAHIM MOHD ALI ALSOFYANI

UNIVERSITI TEKNOLOGI MALAYSIA

OPTIMAL SPEED AND TORQUE ESTIMATIONS FOR IMPROVING THE DTC
DYNAMIC PERFORMANCE OF INDUCTION MACHINES

IBRAHIM MOHD ALI ALSOFYANI

A thesis submitted in fulfilment of the
requirements for the award of the degree of
Doctor of Philosophy (Electrical Engineering)

Faculty of Electrical Engineering
Universiti Teknologi Malaysia

OCTOBER 2014

DEDICATION

To my beloved parents, wife, sons, brothers and sisters

ACKNOWLEDGMENTS

Praise and thanks are due to Allah, and peace and blessings of Allah be upon our prophet, Muhammad and upon all his family and companions. Without help from Allah, I would not be able to accomplish anything in this research work.

I would like to express my sincere gratitude to my supervisor Assoc. Prof. Dr. Nik Rumzi Nik Idris for his continuous support on my Ph.D study, and for his patience, motivation, enthusiasm, and immense knowledge. His guidance has helped me in all the time of research and writing of this thesis. I really appreciate his ethics and great deal of respect with his students.

In addition, I want to thank the Universiti Teknologi Malaysia (UTM), the Ministry of Science, Technology and Innovation (MOSTI) of the Malaysian government for providing the funding for this research. My sincere thanks also go to the Yemen ministry of high education for their partial sponsor and support.

In addition, I am extremely grateful to my parents, my wife Faten Alnadish, my sons Abdulrahman and Almamoun for their unlimited support and encouragement during this research. My sincere appreciation also extends to many people who have contributed to this thesis. Unfortunately, it is not possible to list all of them in this limited space.

ABSTRACT

High-performance AC drives require accurate speed, flux, and torque estimations to provide a proper system operation. Thus, this thesis proposes a robust observer, i.e. Extended Kalman Filter (EKF), to offer optimal estimations of these components in order to improve the dynamic performance of Direct Torque Control (DTC) of induction motor drives. The selection and quality of EKF covariance elements have a considerable bearing on the effectiveness of motor drives. Many EKF-based optimization techniques involve only a single objective for the optimal estimation of speed without giving concern to the other variables. In addition, the optimization is performed on a complicated EKF structure. Nevertheless, in this study, both speed and torque are concurrently estimated. The work presents a new method to investigate the selection of EKF filters by using a Non-Dominated Sorting Genetic Algorithm-II (NSGA-II) developed for resolving problems with multi-objectives. Filter element selection is the process of improving the concurrent estimation of speed and torque in order to increase EKF accuracy and allow higher drive efficiency. The proposed multi-optimal EKF-based estimation observer is used in combination with the sensorless direct torque control of induction motor. The investigated results for the multi-objective optimization indicate that the speed optimization gives superior performance when compared to the optimal torque. Owing to the large computation time of EKF algorithm, it increases the sampling time of DTC which leads to an increase in the motor torque ripples. The thesis proposes a Constant Frequency Torque Controller (CFTC) to replace the hysteresis torque controller that offers constant switching frequency and reduces torque ripples. Moreover, the CFTC has the capability of continuous switching regardless of speed variation; hence, leading to a consistent rotation of flux. Consequently, improvement on speed estimation, particularly at low and zero speed regions is accomplished and enhancement on the dynamic performance of torque is achieved when the reference speed change is applied from 0 rad/s, on the condition that the EKF observer is accurately optimized. To verify the improvements of the proposed methods, simulation and experimentation as well as comparison with the EKF-based DTC with the hysteresis controller are carried out.

ABSTRAK

Pemacu AC berprestasi tinggi memerlukan kelajuan yang tepat, fluks dan jangkaan tork bagi menyediakan suatu operasi sistem yang baik. Maka, tesis ini mencadangkan satu pemerhati yang teguh seperti Penapis Lanjutan Kalman (EKF), untuk menawarkan jangkaan optima komponen ini untuk memperbaiki prestasi dinamik sesuatu Kawalan Tork Langsung (DTC) pemacu motor aruhan. Pemilihan dan kualiti elemen-elemen kovarian EKF mempunyai pengaruh yang besar ke atas keberkesanan pemacu motor. Banyak teknik pengoptimalan berasaskan EKF melibatkan hanya satu objektif tunggal bagi jangkaan optima kelajuan tanpa mengambil kira pembolehubah lain. Tambahan pula, optimasi dijalankan ke atas struktur EKF yang rumit. Tetapi, dalam kajian ini kelajuan dan tork kedua-duanya dianggarkan secara serentak. Kajian membentangkan satu kaedah baru untuk menyelidik pemilihan penapis-penapis EKF dengan menggunakan Algoritma-II Genetik Pengisihan Bukan Dominan (NSGA-II) yang dibangunkan bagi menyelesaikan masalah berkaitan pelbagai objektif. Pemilihan elemen penapis ialah proses memperbaiki jangkaan serentak kelajuan dan tork untuk meningkatkan ketepatan dan meninggikan lagi keberkesanan. Pemerhati jangkaan pelbagai optima berdasarkan EKF diguna bersama dengan pengawalan tork langsung motor aruhan tanpa sensor. Keputusan kajian bagi optimasi pelbagai objektif menunjukkan optimasi kelajuan memberi prestasi lebih baik dibandingkan dengan tork optima. Disebabkan tempoh pengiraan yang lama bagi algoritma EKF, ia meningkatkan masa sampel DTC yang membawa kepada peningkatan dalam riak tork motor. Tesis ini mencadangkan satu Pengawal Frekuensi Tork Tetap (CFTC) untuk menggantikan pengawal tork histerisis yang menawarkan frekuensi pertukaran tetap dan mengurangkan riak tork motor. Disamping itu, CFTC berupaya membuat pertukaran berterusan tanpa menghiraukan perbezaan kelajuan; maka, ini membawa kepada satu putaran fluks yang konsisten. Oleh itu, peningkatan dalam jangkaan kelajuan, khususnya pada bahagian kelajuan rendah dan sifar dicapai dan kemajuan prestasi dinamik tork diperolehi apabila perubahan kelajuan rujukan dihasilkan bila perubahan kelajuan rujukan diaplikasikan daripada 0 rad/s, dengan syarat pemerhati EKF dioptimalkan secara tepat. Bagi mengesahkan penambahbaikan kaedah-kaedah yang disyorkan, simulasi dan eksperimen serta perbandingan dengan DTC berdasarkan EKF dengan pengawal histerisis telah dijalankan.

TABLE OF CONTENTS

CHAPTER	TITLE	PAGE
	DECLARATION	ii
	DEDICATION	iii
	ACKNOWLEDGMENTS	iv
	ABSTRACT	v
	ABSTRAK	vi
	TABLE OF CONTENTS	vii
	LIST OF TABLES	xi
	LIST OF FIGURES	xii
	LIST OF ABBREVIATIONS	xxi
	LIST OF APPENDICES	xxiv
1	INTRODUCTION	1
	1.1 Overview of Induction Motor Drives	1
	1.1.1 Scalar Control	2
	1.1.2 Field Oriented Control (FOC)	4
	1.1.3 Direct Torque Control (DTC)	5
	1.2 Sensorless Control Strategies	6
	1.3 Thesis Objectives and Contributions	7
	1.4 Scope of Research	8
	1.5 Organization of the Thesis	9
2	A REVIEW ON SPEED-SENSORLESS TECHNIQUES	11
	2.1 Introduction	11

2.2	Mathematical Model of Induction Machine	12
	2.2.1 Complex Space Vector Equations	14
	2.2.2 Complex Space Vector Equations	16
2.3	Sensorless Control Strategies	18
	2.3.1 Model Based Estimation Techniques	18
	2.3.1.1 Open Loop Speed Estimation	18
	2.3.1.2 Model Reference Adaptive System	19
	2.3.1.3 Full Order and Reduced Order Closed Loop Observers	21
	2.3.1.4 Extended Kalman Filter	22
	2.3.1.5 Sliding Mode Observer	24
	2.3.1.6 Other Estimation Schemes	26
	2.3.1.7 Difficulties in Model Based Estimation	27
	2.3.2 Estimation through Signal Injection and Parasitic Effects	28
	2.3.2.1 Rotor Slot Tracking	30
	2.3.2.2 Custom Designed or Modified Rotor Slots	30
	2.3.2.3 Saturation Caused by Main Flux	31
2.4	Chapter Conclusion	31
3	OVERVIEW ON THE PRINCIPLES OF DIRECT TORQUE CONTROL AND EXTENDED KALMAN FILTER	32
3.1	Introduction	32
3.2	Basic Principles of Direct Torque Control	32
	3.2.1 3-Phase Voltage Source Inverter Space Vectors	33
	3.2.2 Direct Flux Control	34
	3.2.3 Direct Torque Control	38
	3.2.4 De-coupled Control of Torque and Flux in DTC-hysteresis based Induction Machine	43

3.2.5	Estimation of Flux Using the Low Pass Filter (Voltage Model)	45
3.3	Estimations of Speed, Flux, and Torque Using Extended Kalman Filter (Current Model)	47
3.3.1	Requirements for Speed – Sensorless DTC System of IMs	48
3.3.2	Development of Extended Kalman Filter	48
3.4	Chapter Conclusion	54
4	IMPROVED SPEED-SENSORLESS DIRECT TORQUE CONTROL OF INDUCTION MOTOR USING OPTIMAL EXTENDED KALMAN FILTER	55
4.1	Introduction	55
4.2	The Proposed Non-dominated Sorting Genetic Algorithm II (NSGAI) Optimization Algorithm	57
4.3	Optimizing the EKF Matrices Using NSGA II	58
4.4	Simulation and Experimental Results	65
4.4.1	Simulation of the Proposed Optimal EKF- based DTC	65
4.4.2	Experimental Setup	66
4.4.3	Results and Discussion	68
4.5	Chapter Conclusion	95
5	EKF-BASED DIRECT TORQUE CONTROL WITH A CONSTANT TORQUE FREQUENCY CONTROLLER FOR A WIDE SPEED OPERATION	96
5.1	Introduction	96
5.2	Constant Switching Frequency Controller	97
5.3	Design Procedure of Constant Switching Frequency Controller in DTC	100
5.4	Simulation and Experimental Results	103
5.4.1	Results and Discussion	104
5.5	Chapter Conclusion	139

6	DESCRIPTION OF THE EXPERIMENTAL SET-UP	140
6.1	Introduction	140
6.2	DS1104 Controller Board	142
6.2.1	EKF-based Flux and Torque Estimations	143
6.2.2	Flux Controller	145
6.2.3	Torque Controller	145
6.2.4	Speed Controller	145
6.3	Basys2 Board	145
6.3.1	Voltage Vector Selection Table	146
6.3.2	Blanking Time Generation	147
6.4	Gate Drivers and 3-Phase Voltage Source Inverter (VSI)	149
6.5	The Drive Train Set	151
6.5.1	Induction Motor	152
6.5.2	Torque Transducer	154
6.5.3	Hysteresis Brake	155
6.6	Chapter Conclusions	156
7	CONCLUSION AND FUTURE WORK	157
7.1	Conclusions	157
7.2	Future Work	159
	REFERENCES	161
	Appendices A – E	169-195

LIST OF TABLES

TABLE NO.	TITLE	PAGE
3.1	Voltage vectors selection table as proposed in [10]	45
4.1	DTC-Hysteresis based system and induction machine parameters	71
4.2	The optimum filter parameters based on simulation data for optimum selected points in Pareto optimum front	74
4.3	The optimum filter parameters based on experimental data for optimum selected points in Pareto optimum front	74
6.1	Induction machine parameters	155

LIST OF FIGURES

FIGURE NO.	TITLE	PAGE
1.1	Classification of variable frequency drives for IM control [7]	2
1.2	Closed loop IM with constant V / Hz variable frequency drive	3
1.3	Fundamental direct FOC technique with an observer used for rotor flux estimation	5
1.4	Basic DTC scheme with an observer used for stator flux estimation	6
2.1	Sensorless estimation techniques for induction motor	12
2.2	Cross-section of a single pole-pair three-phase machine	13
2.3	A space vector x in the three-phase symmetric system (based on (2.1))	15
2.4	Model reference adaptive system for speed estimation	20
2.5	Adaptive observer for speed estimation	22
2.6	Structure of extended Kalman filter	25
2.7	Sliding mode observer for speed estimation	26
2.8	FOC drive with speed estimation based on parasitic effects	29
3.1	Schematic diagram of Voltage Source Inverter connected to IM	33
3.2	Voltage space vectors of a 3-phase inverter with the corresponded switching states	34

3.3	Control of flux magnitude using a 2-level hysteresis comparator	35
3.4	Typical waveforms of the stator flux, the flux error and the flux error status for the two-level hysteresis flux comparator	36
3.5	Definition of six sectors of the stator flux plane	37
3.6	Two possible active voltages are switched for each sector to control the stator flux within its hysteresis band	37
3.7	The variation of δ_{sr} with application of (a) active voltage vector, (b) zero or radial voltage vector, (c) reverse voltage vector.	39
3.8	The application of voltage vectors in controlling the δ_{sr} as well as the output torque for 4-quadrant operation	41
3.9	Control of torque using a 3-level hysteresis comparator	43
3.10	Typical waveforms of the torque, the torque error and the torque error status for the three-level hysteresis torque comparator	44
3.11	de-coupled control structure of DTC-hysteresis based induction machine	45
3.12	Structure of extended Kalman filter	53
3.13	Complete structure of EKF-based DTC of IM	54
4.1	The flow program for optimizing EKF using NSGA II	60
4.2	Voltage and current training profiles obtained from simulation for optimizing the EKF parameters using NSGA II	62
4.3	Voltage and current training profiles obtained from experimentation for optimizing the EKF parameters using NSGA II	63
4.4	Speed and torque target profiles obtained from simulation for optimizing the EKF parameters using NSGA II	64

4.5	Speed and torque target profiles obtained from experimentation for optimizing the EKF parameters using NSGA II	64
4.6	SIMULINK blocks of the proposed EKF-based DTC-CSFC	67
4.7	SIMULINK state space model of IM in presence of noise	68
4.8	SIMULINK block of EKF is represented in (a), and the Q and R filters are placed in the K mask (b)	69
4.9	SIMULINK constant switching frequency controller	70
4.10	(a) Experimental Set-up for the EKF-based DTC (b) Implementation of the proposed system drive using DSP and FPGA	70
4.10	Continued	71
4.11	The distribution of Pareto-optimal point solutions for optimizing EKF performance using NSGA-II in two-dimensional spaces based on (a) simulation and (b) experimentation.	73
4.12	Simulation results of NSGA II multi-optimal EKF solutions for the reversed high speed at the minimum speed MSE.	75
4.13	Experimental results of NSGA II multi-optimal EKF solutions for the reversed high speed at the minimum speed MSE.	76
4.14	Experimental results of NSGA II multi-optimal EKF solutions for the reversed high speed at the minimum torque MSE.	77
4.15	Experimental zoomed images (zoomed area indicated by '↔') of NSGA II multi-optimal EKF solutions for the reversed high speed at (a) the minimum speed MSE and (b) the minimum torque MSE.	78
4.16	Simulation results of NSGA II multi-optimal EKF solutions for the low and zero speed at the minimum speed MSE	79

4.17	Experimental results of NSGA II multi-optimal EKF solutions for the low and zero speed at the minimum speed MSE	80
4.18	Experimental results of NSGA II multi-optimal EKF solutions for the low and zero speed at the minimum torque MSE	81
4.19	Experimental zoomed images (zoomed area indicated by '↔') of NSGA II multi-optimal EKF solutions for the low and zero speed at (a) the minimum speed MSE and (b) the minimum torque MSE.	82
4.20	Simulation results of NSGA II multi-optimal EKF solutions for the low speed with 100 % detuning of rotor resistor at the minimum speed MSE.	83
4.21	Experimental results of NSGA II multi-optimal EKF solutions for the low speed with 100 % detuning of rotor resistor at the minimum speed MSE.	84
4.22	Experimental results of NSGA II multi-optimal EKF solutions for the low speed with 100 % detuning of rotor resistor at the minimum torque MSE.	85
4.23	Experimental zoomed images (zoomed area indicated by '↔') of NSGA II multi-optimal EKF solutions for the low speed with 100 % detuning of rotor resistor at (a) the minimum speed MSE and (b) the minimum torque MSE.	86
4.24	Simulation results of NSGA II multi-optimal EKF solutions for the low speed with 50 % detuning of stator resistor at the minimum speed MSE.	87
4.25	Experimental results of NSGA II multi-optimal EKF solutions for the low speed with 50 % detuning of stator resistor at the minimum speed MSE.	88

4.26	Experimental results of NSGA II multi-optimal EKF solutions for the low speed with 50 % detuning of stator resistor at the minimum torque MSE.	89
4.27	Experimental zoomed images (zoomed area indicated by '↔') of NSGA II multi-optimal EKF solutions for the low speed with 50 % detuning of stator resistor at (a) the minimum speed MSE and (b) the minimum torque MSE.	90
4.28	Simulation results of multi-optimal EKF solutions at low reversed speed with a slow triangular motion and applied load at the minimum speed MSE.	91
4.29	Experimental results of multi-optimal EKF solutions at low reversed speed with a slow triangular motion and applied load at the minimum speed MSE.	92
4.30	Experimental results of multi-optimal EKF solutions at low reversed speed with a slow triangular motion and applied load at the minimum torque MSE.	93
4.31	Experimental zoomed images (zoomed area indicated by '↔') of NSGA II multi-optimal EKF solutions for the reversed low speed with applied load at (a) the minimum speed MSE and (b) the minimum torque MSE.	94
5.1	Constant frequency torque controller	99
5.2	Typical waveforms of the constant frequency torque controller	99
5.3	Generated upper triangular waveform using DSP (sampled at $DT \mu s$)	100
5.4	Averaged and linearized torque loop (as proposed in [11])	102
5.5	The generated upper triangle waveform of CSF with a sample time of $120 \mu s$	104
5.6	Bode plot of loop gain with PI controller for the proposed CSFC	105

- 5.7 Simulation comparisons between (a) DTC-HC and (b) DTC-CSFC using EKF observer for step response of speed from 0 rad/s... (1) is speed reference, (2) is estimated speed, (3) is measured speed, (4) is torque reference, (5) is estimated torque, (6) is torque error, (7) is output of PI controller, (8) is lower triangular waveform, and (9) is torque error status. 108
- 5.8 Experimental comparisons between (a) DTC-HC and (b) DTC-CSFC using EKF observer for step response of speed from 0 rad/s... (1) is speed reference, (2) is estimated speed, (3) is measured speed, (4) is torque reference, (5) is estimated torque, (6) is torque error, (7) is output of PI controller, (8) is lower triangular waveform, and (9) is torque error status. 109
- 5.9 Simulation comparisons between (a) DTC-HC and (b) DTC-CSFC using EKF observer for step response of speed from 3.5 rad/s... (1) is speed reference, (2) is estimated speed, (3) is measured speed, (4) is torque reference, (5) is estimated torque, (6) is torque error, (7) is output of PI controller, (8) is lower triangular waveform, and (9) is torque error status. 110
- 5.10 Experimental comparisons between (a) DTC-HC and (b) DTC-CSFC using EKF observer for step response of speed from 3.5 rad/s... (1) is speed reference, (2) is estimated speed, (3) is measured speed, (4) is torque reference, (5) is estimated torque, (6) is torque error, (7) is output of PI controller, (8) is lower triangular waveform, and (9) is torque error status. 111
- 5.11 Simulation comparisons between (a) DTC-HC and (b) DTC-CSFC using EKF observer for step response of speed from 10 rad/s... (1) is speed reference, (2) is estimated speed, (3) is measured speed, (4) is torque reference, (5) is estimated torque, (6) is torque error, (7) is output of PI controller, (8) is lower triangular waveform, and (9) is torque error status. 112

5.12	Experimental comparisons between (a) DTC-HC and (b) DTC-CSFC using EKF observer for step response of speed from 10 rad/s... (1) is speed reference, (2) is estimated speed, (3) is measured speed, (4) is torque reference, (5) is estimated torque, (6) is torque error, and (7) is output of PI controller, (8) is lower triangular waveform, and (9) is torque error status.	113
5.13	Experimental zoomed images (zoomed area indicated by '↔') of the output of PI controller and upper triangular waveform for reference speed change from (a) 0 rad/s, (b) 3.5 rad/s, and (c) 10 rad/s	114
5.14	Simulation results at high reversed speed operation using EKF for DTC-HC.	115
5.15	Experimental results at high reversed speed operation using EKF for DTC-HC.	116
5.16	Simulation results at high reversed speed operation using EKF for DTC-CSFC.	117
5.17	Experimental results at high reversed speed operation using EKF for DTC-CSFC.	118
5.18	Simulation results at low and zero speed operation using EKF for DTC-HC.	119
5.19	Experimental results at low and zero speed operation using EKF for DTC-HC.	120
5.20	Simulation results at low and zero speed operation using EKF for DTC-CSFC.	121
5.21	Experimental results at low and zero speed operation using EKF for DTC-CSFC.	122
5.22	Simulation zoomed images (zoomed area indicated by '↔') of the speed, torque, flux and current (a) waveforms at low and zero speed for DTC-HC.	123

5.23	Experimental zoomed images (zoomed area indicated by '↔') of the speed , torque, flux and current (a) waveforms at low and zero speed for DTC-HC.	124
5.24	Simulation zoomed images (zoomed area indicated by '↔') of the speed , torque, flux and current (a) waveforms at low and zero speed for DTC-CSFC.	125
5.25	Experimental zoomed images (zoomed area indicated by '↔') of the speed, torque, flux and current (a) waveforms at low and zero speed for DTC-CSFC.	126
5.26	Simulation results at slow triangular speed operation using EKF for DTC-HC.	127
5.27	Experimental results at slow triangular speed operation using EKF for DTC-HC.	128
5.28	Simulation results at slow triangular speed operation using EKF for DTC-CSFC.	129
5.29	Experimental results at slow triangular speed operation using EKF for DTC-CSFC.	130
5.30	Simulation results at slow triangular speed operation under load using EKF for DTC-HC.	131
5.31	Experimental results at slow triangular speed operation under load using EKF for DTC-HC.	132
5.32	Simulation results at slow triangular speed operation under load using EKF for DTC-CSFC.	133
5.33	Experimental results at slow triangular speed operation under load using EKF for DTC-CSFC.	134
5.34	Simulation results at high speed operation under step load using EKF for DTC-HC.	135
5.35	Experimental results at high speed operation under step load using EKF for DTC-HC.	136

5.36	Simulation results at high speed operation under step load using EKF for DTC-CSFC.	137
5.37	Experimental results at high speed operation under step load using EKF for DTC-CSFC.	138
6.1	Complete drive system; (a) picture of the experiment set-up, (b) functional block diagram of the experiment set-up...(1) Motor DC power supply, (2) Capacitor, (3) VSI, (4) Current sensor, (5) Oscilloscope, (6) DS1104 Controldesk interface, (7) IM, (8) Torque transducer, (9) Hysteresis brake .	141
6.2	Identifying sectors of the stator flux (a) definition of $\Psi_{sq,1}$, (b) determining sector based on threshold values, i.e. 0 and $\Psi_{sq,1}$	144
6.3	FPGA (Basys2)	146
6.4	Block diagram of voltage vector selection table and blanking time generation using FPGA (Basys2)	148
6.5	Block diagram of blanking time generation for a single leg (i.e. phase a)	148
6.6	Timing diagram of blanking time generation for a single leg (i.e. phase a)	149
6.7	Schematic of the gate driver circuit	150
6.8	Schematic of the IGBT module with the capacitor snubbers	151
6.9	Schematic of the gate driver circuit	151
6.10	Complete drive train couplings (a) picture of the drive train, (b) functional block diagram of the drive train	153
6.10	Continued	154

LIST OF ABBREVIATIONS

<i>AC</i>	-	Alternating Current
<i>ADC</i>	-	Analog to digital converter
<i>B</i>	-	Input matrix
<i>BPF</i>	-	Band pass filter
<i>CFTC</i>	-	Constant Frequency Torque Controller
<i>C_{lower}</i>	-	Lower triangular carrier
<i>C_{p-p}</i>	-	Peak to peak value of the triangular carrier
<i>C_{upper}</i>	-	Upper triangular carrier
<i>d, q</i>	-	Direct and quadrature axis of the stationary reference frame
<i>DAC</i>	-	Digital to analog converter
<i>DC</i>	-	Direct Current
<i>DSP</i>	-	Digital Signal Processor
<i>DTC</i>	-	Direct Torque Control
<i>d^{ψs}, q^{ψs}</i>	-	Direct and quadrature axis of the estimated stator flux reference frame
<i>EKF</i>	-	Extended Kalman filter
<i>emf</i>	-	Electromotive force
<i>f_c</i>	-	Carrier frequency
<i>FOC</i>	-	Field Oriented Control
<i>FPGA</i>	-	Field Programmable Gate Array
<i>I.E</i>	-	Incremental Encoder
<i>I.M</i>	-	Induction Machine
<i>i_{rd}, i_{rq}</i>	-	d and q components of the rotor current in stationary reference frame
<i>i_s, i_r</i>	-	Stator and rotor current space vectors in stationary reference frame
<i>i_{sd}, i_{sq}</i>	-	d and q components of the stator current in stationary reference frame
<i>i_s^g, i_r^g</i>	-	Stator and rotor current space vectors in general reference frame
<i>J</i>	-	Moment of inertia
<i>KF</i>	-	Kalman filter
<i>k_i</i>	-	Integral gain of the PI controller
<i>k_p</i>	-	Proportional gain of the PI controller

L_m	-	Mutual inductance
LPF	-	Low pass filter
L_r	-	Rotor self-inductance
L_s	-	Stator self-inductance
$MRAS$	-	Model reference adaptive system
P	-	Number of pole pairs
$p.p.r$	-	Pulse per revolution
PI	-	Proportional - Integral
PWM	-	Pulse Width Modulation
PWM	-	Pulse-width modulation
$r.m.s$	-	Root mean squared
R_s, R_r	-	Stator and rotor resistance
$S_a, S_b,$ S_c	-	Switching states of phase a, b, c
SI	-	Signal injection
SMO	-	Sliding mode observer
SNR	-	Signal to noise ratio
SVM	-	Space Vector Modulation
T_c	-	Output of PI controller for the CFTC
T_e	-	Electromagnetic torque
$T_{e, rated}$	-	Torque rated
T_e^{ref}	-	Reference torque
T_{stat}	-	Torque error status
t_{tri}	-	Period of C_{upper} or C_{lower}
u	-	Control-input vector
V_{DC}	-	DC link voltage
VFD	-	Variable frequency drives
$VHDL$	-	VHSIC hardware description language
v_s	-	Stator voltage space vector in stationary reference frame
VSD	-	Variable speed drives
v_{sd}, v_{sq}	-	d and q components of the stator voltage in stationary reference frame
v_s^g	-	Stator voltage space vector in general reference frame
VSI	-	Voltage Source Inverter
δ_{sr}	-	Difference angle between stator flux linkage and rotor flux linkage
θ_r	-	Angle with respect to rotor axis
θ_s	-	Angle with respect to stator axis
σ	-	Total flux leakage factor
τ_r	-	Rotor time constant
Ψ_s	-	Estimated stator flux linkage

Ψ_s^g, Ψ_r^g	-	Stator and rotor flux linkage space vectors in general reference frame
Ψ_s, Ψ_r	-	Stator and rotor flux linkage space vectors in stationary reference frame
$\Psi_{sd}^{\psi_s}, \Psi_{sq}^{\psi_s}$	-	d and q components of stator flux in stator flux reference frame
Ψ_{sd}, Ψ_{sq}	-	d and q components of stator flux in stationary reference frame
ω_e	-	Steady state synchronous frequency in rad./s
ω_m	-	Rotor mechanical speed in rad./s
ω_r	-	Rotor electrical speed in rad./s
ω_{slip}	-	Steady state slip frequency in rad./s

LIST OF APPENDICES

APPENDIX NO.	TITLE	PAGE
A	Derivation of torque and flux equations	176
B	Simulation of EKF-based DTC	178
C	EKF MATLAB coding for multi-objective optimization	185
D	DSP source code for EKF-based DTC	188
E	List of publications	202

CHAPTER 1

INTRODUCTION

1.1 Overview of Induction Motor Drives

Induction motors (IMs) dominate the world market (more than 85% of electrical motors)[1] with broad applications in industries, public services and household electrical appliances [2-3]. The popularity of IMs is mainly due to their low cost, ruggedness, high reliability, and minimum maintenance [4]. The induction machines began to gradually replace DC machines in many industrial applications as the Field Oriented Control (FOC) introduced by F. Blachke in 1970's can produce comparable performance to that obtained in DC machines [5]. Moreover, their popularity is also assisted by the rapid development in power semiconductor devices and the emergence of high-speed microprocessor and digital signal processors [6].

Much of the previous research has been devoted to improving the drive systems of the IM, especially the control methodology. The advent of power semiconductor switches and digital control technology has led to remarkable improvements in the variable frequency drives (VFDs) i.e. providing smoother speed tuning, greater motor control, and fewer energy losses. Based on the torque and speed control techniques, the IM-VFDs can be classified into two main categories namely the scalar and vector control methods, as illustrated in Figure 1.1. A brief discussion on these control methods are given as follows.

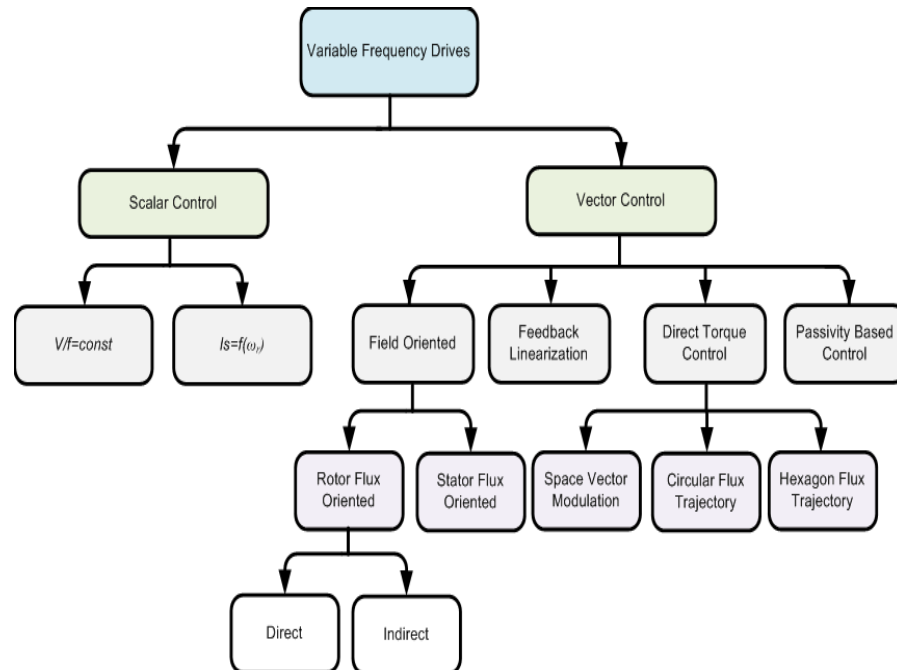


Figure 1.1 Classification of variable frequency drives for IM control [7]

1.1.1 Scalar Control

Scalar control is a simple control technique used to control the speed of complex and nonlinear behavior of the IMs based only on magnitude and frequency of the applied voltages. The control is developed based on a per phase steady-state equivalent circuit of the IM with an objective of maintaining the magnetizing current constant by changing the magnitude of applied voltage proportional to the applied frequency. The magnitude and frequency needed to maintain this constant magnetizing current is then synthesized using a voltage source inverter. An example of a scalar control of IM which is based on a constant ratio of applied voltage to the frequency, widely known as the constant volts per hertz (or constant V/f), is shown in Figure 1.2. For this particular example of control scheme, the speed is controlled in a closed loop manner by measuring the actual speed using a speed sensor. As shown in the figure, the difference between the reference rotor speed value, ω_r^r , and the actual rotor speed, ω_r , which is speed error, is tuned via the conventional

proportional-integral (PI) controller, and a limiter to obtain the slip-speed reference ω_{sl}^r . Then, the slip-speed reference and electrical rotor speed are added together to generate the fundamental stator frequency reference. Thereafter, the fundamental stator frequency reference determines the amplitude of the fundamental stator voltage reference, V_s^r . Without the speed feedback (i.e. open loop constant V/f), the speed regulation will be poor and heavily depends on the mechanical load; nonetheless, for some non-critical applications this is good enough. The inclusion of the speed sensor will increase overall cost of the drive system, but yet the system is still not suitable to be used for applications where precise torque control is mandatory; scalar control is incapable of controlling the most essential variables in IMs, i.e. torque and flux [8]. The main drawbacks of this technique are the unsatisfactory speed accuracy, especially at the low speed regions, and poor torque response. The reaction of the motor to the applied frequency and voltage governs motor flux and torque indirectly based on the steady-state model of the IM [7] which is not valid in transient state. Therefore, for applications requiring precise torque control, vector control schemes are normally adopted as discussed in the next section.

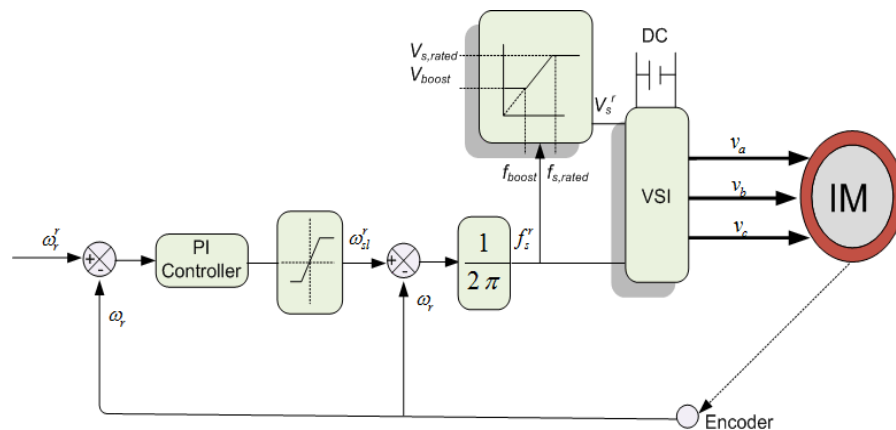


Figure 1.2 Closed loop IM with constant V / Hz variable frequency drive

1.1.2 Field Oriented Control (FOC)

Field oriented control (FOC) or vector control (VC) was introduced by Hasse and Blaschke from Germany, in 1969 and 1971 respectively [7]. On the contrary to the scalar control, the development of FOC control scheme is based on dynamic model of the IM where the voltages, currents and fluxes are expressed in space vector forms. The representation of the motor's quantities using space vectors valid under both steady state and transient conditions hence with FOC, excellent transient response can be achieved. The rotor flux FOC scheme is based on the frame transformation of all quantities to a rotating frame fixed to the rotor flux. In this rotating rotor flux frame, all quantities rotating at synchronous speed will appear as DC quantities. If the flux is aligned to the d axis of this reference frame, it can be shown that the d and q components of the stator current represent the flux and torque component respectively. This means that utilizing FOC, the control of IM is transformed to a simple control scheme similar to the DC motor control where the torque and flux components are decoupled. The way the rotor flux position is obtained determines the type of FOC as either direct FOC or indirect FOC. In indirect FOC, the flux position is obtained by adding the slip position to the measured rotor position, whereas in direct FOC it is calculated (or can also be measured) based on the terminal variables and rotor speed. Figure 1.3 shows the block diagram of a direct rotor flux FOC with speed loop. The rotor speed, which is obtained from the encoder, is used as the speed feedback and also more importantly is used by the observer to calculate the rotor flux position. Alternatively, instead of rotor flux orientation, it is also possible to perform the orientation to the stator flux – which is known as stator flux FOC. It can be seen that in FOC scheme, the knowledge of rotor position need to be acquired accurately in order to perform the frame transformation. Inaccurate rotor flux position causes the torque and flux not to be completely decoupled and consequently resulted in deterioration in the torque dynamics [9].

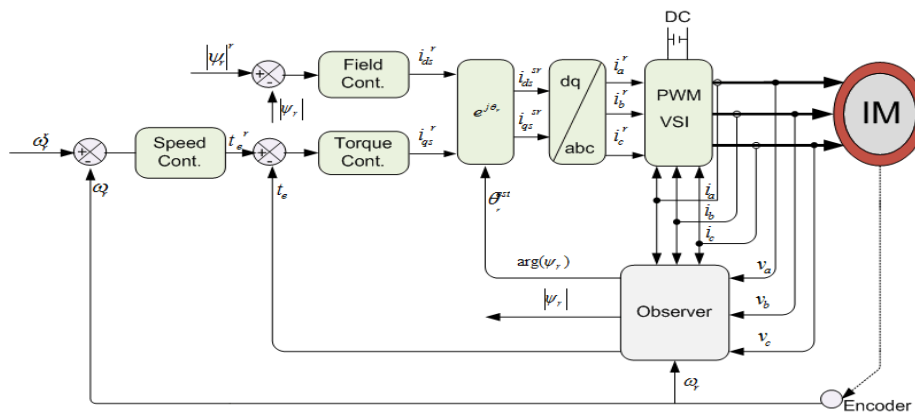


Figure 1.3 Fundamental direct FOC technique with an observer used for rotor flux estimation

1.1.3 Direct Torque Control (DTC)

DTC has become significantly popular and can be considered as an alternative controller to the well-known FOC scheme due to its excellent torque response and its simple control algorithm [10],[11]. The basic structure of DTC of IM scheme is shown in Figure 1.4. The DTC scheme, as initially proposed in [10], consists of a pair of hysteresis comparators, torque and flux calculator, a lookup table, and a voltage-source inverter. The control structure of DTC is much simpler than the FOC system due to the absence of frame transformer, pulse width modulator, and a position encoder. The decouple control of torque and flux is established by selecting appropriate voltage vectors to maintain the torque and flux errors within their hysteresis bands[10]. In DTC, the accuracy of the estimated stator flux is important to ensure correct voltage vector is selected for a decoupled torque and flux control. In its basic configuration, DTC scheme does not require rotor speed information since the estimation of stator flux is performed using voltage-model based observer. However, in order to improve the stator flux estimation at low speed, current-model based observer is normally used, which inevitably require the rotor

speed information. Even if stator flux estimation is performed totally based on voltage-model, the rotor speed is still needed for a speed control system. In other words, rotor speed is one of the important parameters that need to be either measured or estimated to ensure proper DTC scheme implementation. Two of the major issues which are normally addressed in DTC drives are the variation of the switching frequency of the inverter used in the DTC drives with operating conditions and the high torque ripple. It is well known that the source or root to the variable switching frequency problem is the use of hysteresis comparators, in particular, the torque hysteresis comparator [11]. To solve these problems, various implementation schemes are proposed. These include the use of predictive control scheme [12],[13], space vector modulation (SVM) technique [14], artificial intelligence (AI) [15] and constant switching controller [11].

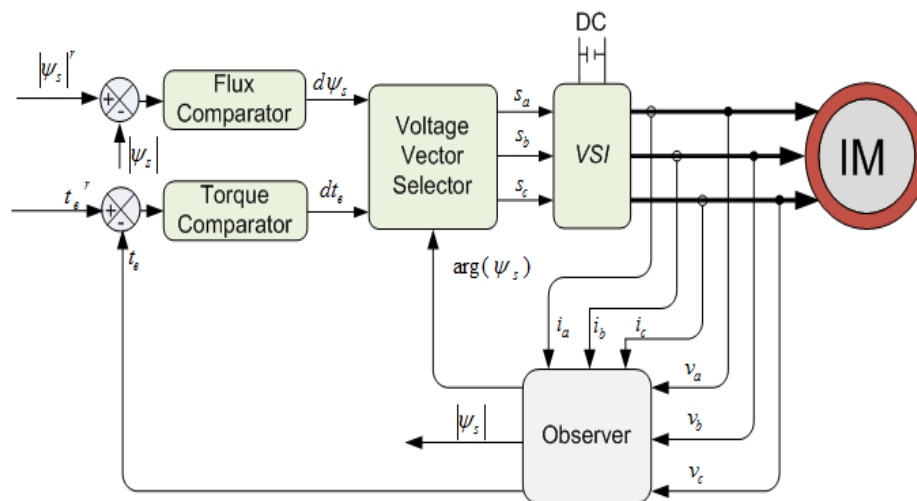


Figure 1.4 Basic DTC scheme with an observer used for stator flux estimation

1.2 Sensorless Control Strategies

Based on the above discussions, regardless of the control strategies used, speed measurement is something essential for control algorithm and/or speed control in the IM drive. The motor speed can be measured using tachometer or optical encoder. However, mechanical speed sensors are associated with several

disadvantages: The increased in the size and cost of the drive system, reduced reliability and robustness, and regular maintenance of the speed sensor itself. Furthermore, in some applications, it is inappropriate to install the mechanical speed encoder at the motor shaft due to the physical and environment constraints. Accordingly, increasing attempts have been made to eliminate the encoder mounted at the motor shaft without affecting the performance of the VFD system. Hence, research interests on sensorless techniques applied to IMs have grown dramatically in the last few decades. Generally, the speed estimation techniques can be classified into two broad categories: Estimation based on mathematical machine model and estimation through signal injection to exploit the anisotropy of the machine as will be discussed in Chapter 2.

1.3 Thesis Objectives and Contributions

The objective of this thesis is to develop a robust estimation method and improve the performance of the speed sensorless DTC of induction motors for a wide speed region, particularly persistent operation at and around zero speed. Despite the improvements, the proposed techniques also aim to retain the simple control structure of DTC drive. The thesis utilizes the simplicity of DTC to propose and implement a powerful estimation technique of extended Kalaman filter (EKF) to achieve a proper induction machine control employed in the DTC with a hysteresis controller (for convenience, it is recognized as EKF-based DTC-HC) and DTC with a constant frequency torque controller (for convenience, it is identified as EKF-based DTC-CSFC) of induction machine i.e. to achieve a speed sensorless drive system, to improve torque dynamic control, and to enhance speed estimation capability for a wide speed operation. While doing the research, the thesis makes the following contributions.

- 1) It offers an alternative method in tuning the EKF for the estimation application of the squirrel cage IM. The main motivation is to reduce the EKF structure complexity by eliminating unnecessary covariance matrices

as well as widening the time scale for the optimization process. Application of the non-dominated sorting genetic algorithm II (NSGA II) method will be carried out to investigate the optimization performance of estimated torque besides the speed estimation. Indeed, this gives a systematic approach in selecting filter solutions with known minimum squared errors (MSEs) for the comparison purpose.

- 2) It analyses the effect of low and zero speed operation on the performance of speed and torque in EKF-based DTC-HC and EKF-based DTC-CSFC drives. Although the DTC is well established to give a high performance torque control, there is still room to further improve the performance based on the observation of the analysis.

1.4 Scope of Research

In order to achieve the objective of the research, the following scope of work has been carried out:

A critical and comprehensive review of speed estimation methods. In this review, the previous works on speed estimation methods used for induction machine drives are addressed. Their strengths and drawbacks based on several evaluation factors are highlighted. Besides giving the overview on the existing estimation methods, the objective of the review is to look for a gap in the literature, particularly on the issue of estimation at low speed region.

Modeling and simulation of the sensorless EKF-based DTC drive. In order to accurately study the sensorless EKF-based DTC of IM, a good model of the induction machine along with the proposed sensorless drive system is required. Thus, the parameters of equivalent circuit of IM are extracted by testing motor under no-load and locked rotor tests. A simple, fast and accurate modeling of overall system is then developed with the usage of MATLAB/SIMULINK software package.

Development of a simple and fast platform to optimize EKF parameters. The EKF was coded in MATLAB instead of using SIMULINK blocks where more time needs to be consumed. Thus, larger time scale has been used to improve on the optimization process.

The proposed speed estimation scheme utilizing a DTC drive have been verified and evaluated for its feasibility and effectiveness through simulation and hardware implementation. A processor and field programmable gate array devices (DS1104 and Xilinx FPGA (Baysis2)) were used to implement the DTC drive including the speed estimation strategy. A standard induction machine with suitable loads and IGBT-based VSI had been used for this purpose.

1.5 Organization of the Thesis

This thesis is organized into seven chapters. Their contents are outlined as follows:

Chapter 2 describes the mathematical modeling of induction machine. Moreover, it provides an extensive review of speed and parameter adaptation techniques. In this review, the recent development of estimation strategies are reviewed based on two categories; mathematical machine model method and estimation via signal injection strategy.

In **Chapter 3**, the basic principle of DTC of induction machines and the state estimator using EKF observer are introduced. It first describes the main components that make the structure of DTC followed with the conventional method (low pass filter) for estimation flux and torque. For the sensorless IM drive, the speed of the motor must be estimated and not measured. Therefore, the EKF algorithm is introduced and discussed.

Chapter 4 presents the optimization process of the EKF based-DTC-CSFC. At the beginning of the chapter, some background materials on the NSGA II and its application on EKF optimization are addressed. Simulation and experimental results on the proposed method are then presented.

Chapter 5 will look at the effect of implementation of EKF on the performance of the DTC-HC and DTC-CSFC for speed estimation at wide speed, including a zero speed region. A quick procedure to design a proper controller of CFTC is presented. Based on the observation, EKF-based DTC-CFTC is able to produce a persistent and stable zero speed operation. Simulation and experimental results are presented to show the effectiveness of the proposed method.

Chapter 6 describes the laboratory experimental set-up to implement the EKF-based DTC. The implementation of the tasks using DS1104 and Xilinx FPGA (Baysis2) are given. Detailed descriptions of each hardware components are provided.

Chapter 7 gives the conclusion of the thesis. Several suggestions are given for possible directions of future work.

the proposed EKF-based DTC-CSFC can give superior dynamic performance when there is a step change from a zero speed zone to higher speed regions. Furthermore, the proposed speed sensorless DTC drive was capable of reducing torque ripple and producing constant switching frequency. The effectiveness of the proposed EKF-based DTC-CSFC in providing wider speed estimation and higher torque capability was verified by simulations and experiments as well as the comparison with the EKF-based DTC with the hysteresis torque controller.

The challenge for EKF experimental implementation is the derivation of the Jacobian matrices which require sufficiently small time intervals for linearization. In order to achieve small step intervals, some of the main tasks of the DTC (i.e. look-up table and blanking time) are implemented utilizing a Xilinx FPGA (Baysis2), this way; the DSP (DSPACE 1104) is able to execute the EKF-based DTC algorithm including the CSFC at the minimum sampling period of 120 μ s.

7.2 Future Work

In this thesis, several contributions are presented. However, there remain potentially new findings in the area of EKF optimization and EKF-based DTC control that can still be explored. These can be summarized in the following section.

- a) **Incorporating the parameter compensation.** In spite of the robustness of the EKF filter against parameter variations, the robustness comes to an end at a certain value. Therefore, it is suggested to incorporate parameter adaptation to compensate for the parameter variation which leads to more stability of the proposed drive system.
- b) **Performing the CFSC and flux hysteresis calculation in the FPGA.** The triangular waveforms for the proposed CSFC are generated by the DSPACE 1104 with a sampling period of 120 μ s.

Since the triangular waveform is generated by software, its frequency and the torque loop bandwidth are restricted by the sampling time of the DSP controller. Enlargement of the triangular frequency can be achieved if the CFSC is performed in the FPGA with higher frequency leading to great reduction of torque ripple. In addition, this can enhance the linearization of Jacobian matrices of EKF by achieving smaller step intervals; hence, enhancing the stability of EKF and improving the estimation of flux, torque, and speed.

- c) **Replacing the hysteresis based flux controller with a fixed switching frequency controller.** In this thesis, the proposed method only utilizes the CSFC for the torque loop. In order for the stator flux error switching to be independent of the speed variation, it is suggested to replace the flux hysteresis comparator of DTC with CSFC.

- d) **Applying other multi-objective swarm and evolutionary optimization techniques for EKF filter tuning.** In the current work, non-dominated sorting genetic algorithm II (NSGA II) was used to optimize the EKF filter parameters for speed and torque estimations. However, there are still other multi-objective techniques that have not been exploited for EKF tuning purpose. It would be exciting to explore the optimization capabilities of other techniques and then to be compared with NSGA II. Additionally, multi-objective can be applied not only for speed and torque, but can be used for speed and stator and rotor resistor optimization.

REFERENCES

1. Saravanan, C., J. Sathiswar and S. Raja, *Performance of Three Phase Induction Motor using Modified Stator Winding*. International Journal of Computer Applications, 2012. 46(1): 1-4.
2. Chakraborty, A., *Advancements in power electronics and drives in interface with growing renewable energy resources*. Renewable and Sustainable Energy Reviews, 2011. 15(4): 1816-1827.
3. Saidur, R., S. Mekhilef, M.B. Ali, A. Safari and H.A. Mohammed, *Applications of variable speed drive (VSD) in electrical motors energy savings*. Renewable and Sustainable Energy Reviews, 2012. 16(1): 543-550.
4. Amjad, S., S. Neelakrishnan and R. Rudramoorthy, *Review of design considerations and technological challenges for successful development and deployment of plug-in hybrid electric vehicles*. Renewable and Sustainable Energy Reviews, 2010. 14(3): 1104-1110.
5. Blaschke, F., *The Principle of Field-Oriented Control as applied to the New Transvector Closed-Loop Control System for Rotating-Field Machines*. Siemens Review, 1972. 34: 217-220.
6. Gabriel, R. and W. Leonhard, *Microprocessor control of induction motor.*, in *Proc. IEEE-IAS Int Semiconductor Power Conv Conf.* 1982. p. 538-545.
7. Buja, G.S. and M.P. Kazmierkowski, *Direct torque control of PWM inverter-fed AC motors - a survey*. IEEE Transactions on Industrial Electronics, 2004. 51(4): 744-757.
8. Martins, C.A. and A.S. Carvalho. *Technological trends in induction motor electrical drives*. in IEEE Porto Power Tech Proceedings. 2001.
9. Vas, P., *Sensorless Vector and Direct Torque Control*. 1998, New York: Oxford Univ. Press.

10. Takahashi, I. and T. Noguchi, *A New Quick-Response and High-Efficiency Control Strategy of an Induction Motor*. IEEE Trans. Ind. App., 1986. IA-22(5): 820-827.
11. Idris, N.R.N. and A.H.M. Yatim, *Direct torque control of induction machines with constant switching frequency and reduced torque ripple*. IEEE Trans. Ind. Electron., 2004. 51(4): 758-767.
12. Geyer, T., G. Papafotiou and M. Morari, *Model Predictive Direct Torque Control—Part I: Concept, Algorithm, and Analysis*. IEEE Trans. Ind. Electron., 2009. 56(6): 1894-1905.
13. Geyer, T., *Computationally Efficient Model Predictive Direct Torque Control*. IEEE Trans. Power Electron., 2011. 26(10): 2804-2816.
14. Gholinezhad, J. and R. Noroozian. *Application of cascaded H-bridge multilevel inverter in DTC-SVM based induction motor drive*. in Proc. Int. Conf. Power Electronics and Drive Systems Technology. 2012.
15. Mir, S. and M.E. Elbuluk. *Precision torque control in inverter-fed induction machines using fuzzy logic*. in Proc. Int. Conf. Power Electronics Specialists. 1995.
16. Holtz, J., *Sensorless Control of Induction Machines; With or Without Signal Injection?* IEEE Trans. Ind. Electron., 2006. 53(1): 7-30.
17. Gadoue, S.M., D. Giaouris and J.W. Finch, *Sensorless Control of Induction Motor Drives at Very Low and Zero Speeds Using Neural Network Flux Observers*. IEEE Transactions on Industrial Electronics, 2009. 56(8): 3029-3039.
18. Finch, J.W. and D. Giaouris, *Controlled AC Electrical Drives*. IEEE Trans. Ind. Electron., 2008. 55(2): 481-491.
19. Leonhard, W., *Control of Electrical Drives*. 1984, Berlin: Springer-Verlag.
20. Bose, B.K., *Power Electronics and AC Drives*. 1986, New Jersey: Prentice-Hall.
21. Murphy, J.M.D. and F.G. Turnbull, *Power Electronic Control of AC Motors*. 1987, Oxford: Pergamon Press.
22. M. Barut, S. Bogosyan and M. Gokasan, *Experimental Evaluation of Braided EKF for Sensorless Control of Induction Motors*. IEEE Transaction on Industrial Electronics, 2008. 55(2): 620-632.

23. Maurizio, C., P. Marcello, C. Giansalvo and C. Grard-Andr, *Sensorless Control of Induction Machines by a New Neural Algorithm: The TLS EXIN Neuron*. IEEE Transactions on Industrial Electronics, 2007. 54(1): 127-149.
24. Fang-Zheng, P. and T. Fukao, *Robust speed identification for speed-sensorless vector control of induction motors*. IEEE Transactions on Industry Applications, 1994. 30(5): 1234-1240.
25. Maiti, S., C. Chakraborty, Y. Hori and M.C. Ta, *Model Reference Adaptive Controller-Based Rotor Resistance and Speed Estimation Techniques for Vector Controlled Induction Motor Drive Utilizing Reactive Power*. IEEE Transactions on Industrial Electronics, 2008. 55(2): 594-601.
26. Karanayil, B., M.F. Rahman and C. Grantham, *An implementation of a programmable cascaded low-pass filter for a rotor flux synthesizer for an induction motor drive*. IEEE Trans. Power Electron., 2004. 19(2): 257-263.
27. Li, Y. and W. Qin. *Low speed performance improvement of sensorless IM control system based on MRAS and NN flux observers*. in IEEE International Conference on Intelligent Computing and Intelligent Systems (ICIS). 2010.
28. Orłowska-Kowalska, T. and M. Dybkowski, *Stator-Current-Based MRAS Estimator for a Wide Range Speed-Sensorless Induction-Motor Drive*. IEEE Transactions on Industrial Electronics, 2010. 57(4): 1296-1308.
29. Rashed, M., F. Stronach and P. Vas. *A new stable MRAS-based speed and stator resistance estimators for sensorless vector control induction motor drive at low speeds*. in 38th Industry Applications Conference, IAS Annual Meeting. 2003.
30. Ravi Teja, A.V., C. Chakraborty, S. Maiti and Y. Hori, *A New Model Reference Adaptive Controller for Four Quadrant Vector Controlled Induction Motor Drives*. IEEE Transactions on Industrial Electronics, 2012. 59(10): 3757-3767.
31. Gadoue, S.M., D. Giaouris and J.W. Finch. *A new fuzzy logic based adaptation mechanism for MRAS sensorless vector control induction motor drives*. in 4th IET Conference on Power Electronics, Machines and Drives. 2008.
32. Sayouti, Y., A. Abbou, M. Akherraz and H. Mahmoudi. *Sensor less low speed control with ANN MRAS for direct torque controlled induction motor*

- drive*. in International Conference on Power Engineering, Energy and Electrical Drives (POWERENG). 2011.
33. Gadoue, S.M., D. Giaouris and J.W. Finch, *MRAS Sensorless Vector Control of an Induction Motor Using New Sliding-Mode and Fuzzy-Logic Adaptation Mechanisms*. IEEE Transaction on Energy Conversion, 2010. 25(2): 394-402.
 34. Cirrincione, M., M. Pucci, G. Cirrincione and G.A. Capolino, *An adaptive speed observer based on a new total least-squares neuron for induction machine drives*. IEEE Transaction on Industry application, 2006. 42(1): 89-104.
 35. Davari, S.A., D.A. Khaburi, W. Fengxiang and R.M. Kennel, *Using Full Order and Reduced Order Observers for Robust Sensorless Predictive Torque Control of Induction Motors*. IEEE Transactions on Power Electronics, 2012. 27(7): 3424-3433.
 36. Harnefors, L. and M. Hinkkanen, *Complete Stability of Reduced-Order and Full-Order Observers for Sensorless IM Drives*. IEEE Transactions on Industrial Electronics, 2008. 55(3): 1319-1329.
 37. Kubota, H., K. Matsuse and T. Nakano, *DSP-based speed adaptive flux observer of induction motor*. IEEE Transactions on Industry Applications, 1993. 29(2): 344-348.
 38. Salmasi, F.R. and T.A. Najafabadi, *An Adaptive Observer With Online Rotor and Stator Resistance Estimation for Induction Motors With One Phase Current Sensor*. IEEE Trans. Energy Convers., 2011. 26(3): 959-966.
 39. Barut, M., R. Demir, E. Zerdali and R. Inan, *Real-Time Implementation of Bi Input-Extended Kalman Filter-Based Estimator for Speed-Sensorless Control of Induction Motors*. IEEE Trans. Ind. Electron., 2012. 59(11): 4197-4206.
 40. Buyamin, S. and J.W. Finch. *Comparative Study on Optimising the EKF for Speed Estimation of an Induction Motor using Simulated Annealing and Genetic Algorithm*. in IEEE Proc. IEMDC Conf. . 2007.
 41. Alsofyani, I.M., N.R.N. Idris, T. Sutikno and Y.A. Alamri. *An optimized Extended Kalman Filter for speed sensorless direct torque control of an induction motor*. in Proc. Int. Power and Energy 2012.

42. Ozsoy, E.E., M. Gokasan and S. Bogosyan, *Simultaneous rotor and stator resistance estimation of squirrel cage induction machine with a single extended kalman filter*. Turkish Journal of Electrical Engineering and Computer Sciences, 2010. 18(5): 853-863.
43. Gherram, K., K. Yazid and M. Mena. *Sensorless indirect vector control of an induction motor by ANNs observer and EKF*. in 18th Mediterranean Conference on Control & Automation (MED). 2010.
44. Danan, S., L. Wenli, D. Lijun and L. Zhigang. *Speed Sensorless Induction Motor Drive Based on EKF and G-I Model*. in International Conference on Computer Distributed Control and Intelligent Environmental Monitoring (CDCIEM). 2011.
45. Lascu, C., I. Boldea and F. Blaabjerg, *Very-low-speed variable-structure control of sensorless induction machine drives without signal injection*. IEEE Transactions on Industry Applications, 2005. 41(2): 591-598.
46. Hajian, M., G.R. Arab Markadeh, J. Soltani and S. Hoseinnia, *Energy optimized sliding-mode control of sensorless induction motor drives*. Energy Conversion and Management, 2009. 50(9): 2296-2306.
47. Comanescu, M., *An Induction-Motor Speed Estimator Based on Integral Sliding-Mode Current Control*. IEEE Transactions on Industrial Electronics, 2009. 56(9): 3414-3423.
48. Derdiyok, A., *Speed-Sensorless Control of Induction Motor Using a Continuous Control Approach of Sliding-Mode and Flux Observer*. IEEE Transactions on Industrial Electronics, 2005. 52(4): 1170-1176.
49. Ghanes, M. and Z. Gang, *On Sensorless Induction Motor Drives: Sliding-Mode Observer and Output Feedback Controller*. IEEE Transactions on Industrial Electronics, 2009. 56(9): 3404-3413.
50. Vieira, R.P., C.C. Gastaldini, R.Z. Azzolin and H.A. Grundling. *Discrete-time sliding mode approach for speed estimation of symmetrical and asymmetrical induction machines*. in 37th Annual Conference on IEEE Industrial Electronics Society IECON. 2011.
51. Yongchang, Z., Z. Jianguo, X. Wei, H. Jiefeng, D.G. Dorrell and Z. Zhengming. *Speed sensorless stator flux oriented control of three-level inverter-fed induction motor drive based on fuzzy logic and sliding mode*

- control.* in 36th Annual Conference on IEEE Industrial Electronics Society IECON. 2010.
52. Zaky, M.S., M. Khater, H. Yasin and S.S. Shokralla, *Very low speed and zero speed estimations of sensorless induction motor drives.* Electric Power Systems Research, 2010. 80(2): 143-151.
 53. Zaky, M.S., M.M. Khater, S.S. Shokralla and H.A. Yasin, *Wide-Speed-Range Estimation With Online Parameter Identification Schemes of Sensorless Induction Motor Drives.* IEEE Transactions on Industrial Electronics, 2009. 56(5): 1699-1707.
 54. Bolognani, S., L. Peretti and M. Zigliotto, *Parameter Sensitivity Analysis of an Improved Open-Loop Speed Estimate for Induction Motor Drives.* IEEE Transactions on Power Electronics, 2008. 23(4): 2127-2135.
 55. Boussak, M. and K. Jarray, *A high-performance sensorless indirect stator flux orientation control of induction motor drive.* IEEE Transactions on Industrial Electronics, 2006. 53(1): 41-49.
 56. de Santana, E.S., E. Bim and W.C. do Amaral, *A Predictive Algorithm for Controlling Speed and Rotor Flux of Induction Motor.* IEEE Transactions on Industrial Electronics, 2008. 55(12): 4398-4407.
 57. Toliyat, H.A., M. Wlas and Z. Krzemiriski, *Neural-Network-Based Parameter Estimations of Induction Motors.* IEEE Trans. Ind. Appl., 2008. 55(4): 1783-1794.
 58. Guanghai, W., H.F. Hofmann and A. El-Antably, *Speed-sensorless torque control of induction machine based on carrier signal injection and smooth-air-gap induction machine model.* IEEE Transactions on Energy Conversion, 2006. 21(3): 699-707.
 59. Giaouris, D., J.W. Finch, O.C. Ferreira, R.M. Kennel and G.M. El-Murr, *Wavelet Denoising for Electric Drives.* IEEE Transactions on Industrial Electronics, 2008. 55(2): 543-550.
 60. Garcia, P., F. Briz, M.W. Degner and D. Diaz-Reigosa, *Accuracy, Bandwidth, and Stability Limits of Carrier-Signal-Injection-Based Sensorless Control Methods.* IEEE Transactions on Industry Applications, 2007. 43(4): 990-1000.

61. Pineda-Sanchez, M., M. Riera-Guasp, J.A. Antonino-Daviu, J. Roger-Folch, J. Perez-Cruz and R. Puche-Panadero, *Diagnosis of Induction Motor Faults in the Fractional Fourier Domain*. IEEE Transactions on Instrumentation and Measurement, 2010. 59(8): 2065-2075.
62. McNamara, D.M., B. Enayati and A.K. Ziarani. *Sensorless speed measurement of induction motors using an adaptive frequency-tracking algorithm*. in 34th Annual Conference of IEEE Industrial Electronics IECON 2008.
63. Keysan, O. and H. Bulent Ertan. *Higher order rotor slot harmonics for rotor speed & position estimation*. in 12th International Conference on Optimization of Electrical and Electronic Equipment (OPTIM). 2010.
64. Staines, C.S., G.M. Asher and M. Sumner, *Rotor-position estimation for induction machines at zero and low frequency utilizing zero-sequence currents*. IEEE Transactions on Industry Applications, 2006. 42(1): 105-112.
65. Zhi, G., T.G. Habetler, R.G. Harley and R.S. Colby, *A Sensorless Rotor Temperature Estimator for Induction Machines Based on a Current Harmonic Spectral Estimation Scheme*. IEEE Transactions on Industrial Electronics, 2008. 55(1): 407-416.
66. Degner, M.W. and R.D. Lorenz, *Using multiple saliencies for the estimation of flux, position, and velocity in AC machines*. IEEE Transactions on Industry Applications, 1998. 34(5): 1097-1104.
67. Jansen, P.L. and R.D. Lorenz, *Transducerless position and velocity estimation in induction and salient AC machines*. IEEE Transactions on Industry Applications, 1995. 31(2): 240-247.
68. Holtz, J. *Sensorless control of induction motors-performance and limitations*. in Proceedings of the 2000 IEEE International Symposium on Industrial Electronics (ISIE). 2000.
69. Jung-Ik, H. and S. Seung-Ki. *Sensorless field orientation control of an induction machine by high frequency signal injection*. in Thirty-Second Industry Applications Conference, IAS Annual Meeting. 1997.
70. Jung-Ik, H. and S. Seung-Ki. *Physical understanding of high frequency injection method to sensorless drives of an induction machine*. in Industry Applications Conference. 2000.

71. Purcell, A. and P. Acarnley, *Device switching scheme for direct torque control*. Electronics Letters, 1998. 34(4): 412-414.
72. Bird, I.G. and H. Zelaya-De La Parra, *Fuzzy logic torque ripple reduction for DTC based AC drives*. Electronics Letters, 1997. 33(17): 1501-1502.
73. MAYBECK, P.S., *Stochastic Models, Estimation and Control*. Vol. 141-1. 1979: Academic Pres.
74. KALMAN, R.E., *A new approach to linear filtering and prediction problems*. Journal of Basic Engineering, 1960. 82(D): 35-45.
75. GREWAL, M.S. and A.P. ANDREWS, *Kalman Filtering : theory and practice using MATLAB*. 2001, New York: Wiley.
76. Alsofyani, I.M. and N.R.N. Idris, *A review on sensorless techniques for sustainable reliability and efficient variable frequency drives of induction motors*. Renewable and Sustainable Energy Reviews, 2013. 24(0): 111-121.
77. Shi, K.L., T.F. Chan, Y.K. Wong and S.L. Ho, *Speed estimation of an induction motor drive using an optimized extended Kalman filter*. IEEE Trans. Ind. Electron., 2002. 49(1): 124-133.
78. Winston, W., *Operations Research: Applications and Algorithms*. 1994, Belmont, California: Duxbury Press.
79. Deb, K., A. Pratap, S. Agarwal and T. Meyarivan, *A fast and elitist multiobjective genetic algorithm: NSGA-II*. IEEE Transactions on Evolutionary Computation, 2002. 6(2): 182-197.
80. Barut, M., S. Bogosyan and M. Gokasan, *Speed-Sensorless Estimation for Induction Motors Using Extended Kalman Filters*. IEEE Trans. Ind. Electron., 2007. 54(1): 272-280.
81. Barut, M., S. Bogosyan and M. Gokasan, *Experimental Evaluation of Braided EKF for Sensorless Control of Induction Motors*. IEEE Trans. Ind. Electron., 2008. 55(2): 620-632.